Modeling of the Branching Point Distribution During the Polymerization of *N*-Vinylpyrrolidone

Stefan Welzel,* Christian Zander, Klaus-Dieter Hungenberg, and Ulrich Nieken

To gain insights into the microstructure of polyvinylpyrrolidone (PVP), a detailed reaction mechanism is developed, which characterizes the polymer along the property coordinate chain length, terminal double bonds (TDB), and branching points. For practical purposes, calculations with three property coordinates are unfeasible, and model reduction is needed. Here, a reduced model with only one single property coordinate without significant loss of accuracy is derived. In the first step, the coordinate TDBs are reduced by a linear relationship between TDBs and chain length. As the parameters of this relation are state dependent, they are dynamically adjusted from a parallel calculated 0D model. In a second step, the pseudodistribution approach is used to reduce the 2D distribution to chain length as the only property coordinate and calculate moments of branching points as a function of chain length. A 2D class model is set up for validation. To demonstrate the benefits of the model, the chain length distribution and moments of branching points are calculated for different average residence times and monomer concentrations in a stirred tank reactor. In a future publication, the model will be validated by experimental data in terms of chain length distribution and branching points.

1. Introduction

Specialty polymers, such as polyvinylpyrrolidone (PVP), are mainly produced in batch or semibatch operated tank reactors. The main advantage of this process type is its flexibility due to the demand of varying quantities. In the sense of process intensification, continuously operated reactor systems have been considered due to better controllability, higher energy efficiency, and improved heat transfer. In particular, tubular reactors with

S. Welzel, C. Zander, U. Nieken
Universität Stuttgart
Institut für Chemische Verfahrenstechnik
Böblinger Str. 78, Stuttgart 70199, Germany
E-mail: stefan.welzel@icvt.uni-stuttgart.de

K.-D. Hungenberg
Hungenberg Consultant
Ortsstrasse 135, Birkenau 69488, Germany

mixing elements are of interest to produce low-volume products such as PVP. A serious problem for the polymerization of N-vinylpyrrolidone (NVP) in continuously operated mixer reactors is the formation of fouling deposits, which result in blocking and shutdown. Side reactions that produce high molecular weight, branched, or even cross-linked polymer chains are considered a prerequisite for fouling. Local back-mixing and stagnant flow in dead zones increase the local residence time and enhance the formation of a polymer network.[1–3] To predict the onset of fouling in static mixer reactors, kinetic models, which provide information about the microstructure of the polymers, are essential. In the first step, we develop a model for well-defined hydrodynamic conditions in a CSTR. The variation in the average residence time gives a first approximation of the behavior in stagnant regions of mixing elements in continuously operated reactors.

The reaction mechanism of NVP polymerization has been studied extensively. The propagation rate coefficient[4,5] and the termination rate coefficient[6] in aqueous solution were determined using pulsed-laser polymerization in conjunction with polymer analysis by size-exclusion chromatography. Transfer to monomers has been studied in Refs. [1] and [7]. Transfer reactions to the solvent seem to be the dominant termination reaction in organic solutions, while termination by combination dominates termination in aqueous solution.[8] In previous work,[9] the formation of terminal double bonds (TDBs) by transfer to monomers and subsequent propagation of TDBs was identified as the main reason for long chain branching in aqueous NVP polymerization. In a recent publication, a model for the number of terminal double bonds was developed, which was successfully validated against experimental data from CSTR experiments.[10]

The full scheme of kinetic reactions for aqueous radical polymerization of NVP (**Table 1**) characterizes a PVP chain by three discrete property coordinates: the chain length, the number of terminal double bounds (TDB), and the number of branching points (BP). Rigorous treatment is practically impossible, and model reduction is needed. In this work, we extend the approach of Zander et al.[10] and derive a 1D model for the chain length and the number of branching points as a function of chain length. Parameters, which are required for model reduction, are updated dynamically, which improves predictions during transient

Table 1. Set of reactions for the polymerization of N-vinylpyrrolidone in aqueous solution with chain length (n,m), number of terminal double bonds (i,j), and number of branching points (k,l).[9]

Initiator dissociation/Initiation	$I_2 \xrightarrow{k_d} 2f_d I / I + M \xrightarrow{k_p} R_{1,0,0}$
Propagation	$R_{n,i,k} + M \xrightarrow{k_p} R_{n+1,i,k}$
Termination by recombination	$R_{n,i,k} + R_{m,j,l} \xrightarrow{k_{t,c}} P_{n+m,i+j,k+l}$
Transfer to monomer	$R_{n,i,k} + M \xrightarrow{k_{tr,M}} P_{n,i,k} + R_{1,1,0}$
Propagation of terminal double bonds	$R_{n,i,k} + P_{m,j,l} \xrightarrow{j \cdot k_{p,TDB}} R_{n+m,i+j-1,k+l+1}$

reactor operation. To validate the modeling approach, we compare the results to a computationally expensive class model.

In the last part, we show the impact of residence times and monomer concentrations on the branching point distribution in a CSTR.

2. Reaction Scheme

The set of reactions for the polymerization of *N*-vinylpyrrolidone in aqueous solution, which was identified in Ref. [9], is summarized in Table 1. The dead species are defined as *P*, and the living species are defined as *R*. Three different property coordinates are taken into account: chain length (n,m), number of terminal double bonds (i,j), and number of branching points (k,l). In addition to classical reactions for radical polymerization, such as initiation, propagation, and termination, there are important side reactions (**Figures 1–3**), which are the reason for the formation of branching points.

The transfer to monomer reaction generates a terminal double bond (TDB) due to transfer of the radical (red) to a monomer molecule by H-abstraction, as illustrated in Figure 1. Figure 2 shows the propagation of terminal double bonds, which consumes one TDB and produces one branching point (BP). By the formation and propagation of terminal double bonds, highly branched molecules are generated, as sketched in Figure 3. While propagation of monomer units does not affect the number of terminal double bonds and branching points, termination by combination reaction adds up the number of TDB, BP as well as the chain length. The rate of propagation of terminal double bonds is proportional to the number of TDBs in a polymer molecule. This makes the reaction schema nonlinear. Thus, moment equations do not close, and a closure condition is needed. To avoid a further
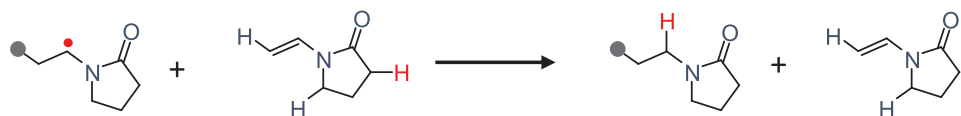
increase in complexity, the formation of multiradicals has been neglected. The kinetic coefficients for all reactions are listed in **Table 2**.

3. Model Development

Rigorous simulations with three property coordinates (chain length, terminal double bonds, branching points) are practically infeasible. Therefore, the problem needs to be reduced into 1D problems along one single property coordinate, which can be solved, for example, by Predici.

Here, we extend the work of Zander[10] and develop a model that allows to calculate the full chain length distribution and the average number of branching points as a function of chain length. The model developed in Ref. [10] is briefly summarized in Section 3.2. As shown in Ref. [10], there is a linear correlation between the average number of TDBs and the chain length. This allows to eliminate the number of terminal double bonds as an independent property coordinate by calculating the moments of this property coordinate and using the linear correlation as a closure relation. Parameters of this closure relation (slope (A) and axis intercept (B)) can be calculated from a computationally cheap moment model, which is termed the "TDB double moment model" in Ref. [10]. Model designation is kept for convenience. The 2D model (chain length, branching points) can be further reduced by calculating the moments of the branching points. This step is detailed in Section 3.3. Finally, one obtains a set of 1D models: the chain length distribution of dead and living polymers and the moments of the branching point distribution as a function of chain length. Since the parameters of the linear correlation between chain length and average number of terminal double bonds (TDB) are propagated during model reduction, source terms of the reduced model are functions thereof. By simultaneous calculation of the "TDB double moment model" and the 1D models, the parameters of the linear correlation (A, B) are updated dynamically, and the model can be used for transient simulations without any adaptation. **Figure 4** shows an overview of the model reduction.

To validate the reduced model, a comparison with a 2D model (class model) is conducted. The class model is briefly introduced in Section 3.4. and a comparison of simulation results are discussed in Section 3.5. The parameters of a reference case for simulations are given in **Table 3**. These conditions are typical for the

Figure 1. Transfer to monomer reaction scheme. The radical center (red dot) is transferred to a monomer molecule. Adapted from Ref. [9].
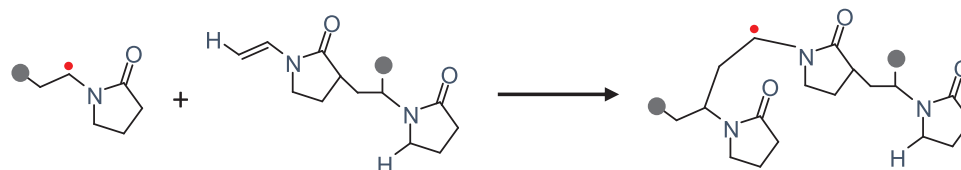

Figure 2. Propagation of terminal double bonds (TDBs) for polymer chains with one TDB. Adapted and simplified from Ref. [9].
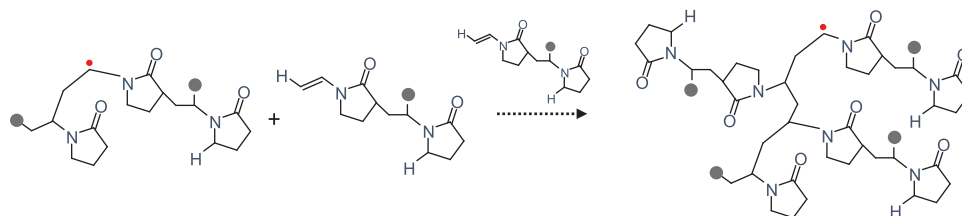
Figure 3. The propagation reaction of terminal double bonds allows the formation of highly branched molecules.

Table 2. Kinetic coefficients for the reaction system of N-vinylpyrrolidone.

Kinetic coefficients	
$k_d/s^{-1} = 9.17 \times 10^{14} \exp\left(\frac{-1.49 \times 10^4}{(T/K)}\right)$	[7]
$\frac{k_p}{k_{p,max}} = 0.36 + 0.64 \exp(-9.2 w_{NVP}) - 0.31 w_{NVP}$	[4]
with	
$k_{p,max}/(L \cdot mol^{-1} \cdot s^{-1}) = 2.57 \times 10^7 \exp\left(\frac{2.12 \times 10^3}{(T/K)}\right)$	
$\frac{k_t}{L \cdot mol^{-1} \cdot s^{-1}} = \left(\frac{1}{k_{SD}} + \frac{\eta}{k_{TD}}\right)^{-1} + k_{RD}$	[11]
with	
$\frac{k_{SD}(p)}{L \cdot mol^{-1} \cdot s^{-1}} = \left(4.87 \times 10^7 \exp\left(-\frac{w_{NVP}}{0.29}\right) + 5.47 \times 10^6\right) \cdot$	
$\exp\left(-5.61 \times 10^{-4} \left(\frac{p}{bar} - 2000\right)\right)$	
$k_{TD} = 31 k_{SD}$	
$\eta = \exp(14.75 w_{PVP})$	
$k_{RD} = 140 w_{NVP} k_p$	
with the mass fraction w_{NVP} for NVP resp. w_{PVP} for PVP and the viscosity η.	
$\frac{k_{tr,m}}{k_p} = 6 \cdot 10^{-4}$	[7]
$\frac{k_{p,TDB}}{L \, mol^{-1} \, s^{-1}} = 3300$	[10]
$f_d = 0.7$	[7]

polymerization of NVP in aqueous solution. An isothermal CSTR is used as the reactor setup.

3.1. Reduction of Property Coordinate "Terminal Double Bonds"

The full set of reactions listed in Table 1 spans three dimensions in property space, with coordinates chain length, terminal double bonds (TDB), and branching points (BP). As already mentioned, the propagation rate of TDBs depends on the number of TDBs, while the number of branching points does not enter the rate expressions. Zander[10] therefore investigated the kinetic model with the property coordinates chain length and TDB's only and found that the average number of TDB's and the chain length are linearly correlated. Polymer chains of length (m) thus exhibit an average number of TDBs, $p(m)$, according to Equation (1):

$$p(m) = A \cdot m + B \tag{1}$$

with parameters A and B. Making use of this relation as a closing condition and forming the moments on the number of TDB allows the removal of the property coordinate "terminal double bonds." To determine the parameters A and B, a (0D) moment model was formulated. We summarize this approach in the following subsection.

3.2. Moment model for the number of TDB

To obtain averaged information on the number of terminal double bonds, a moment model is derived by taking the moments of all property coordinates. This results in a set of differential equations for the moments and can be solved with minimal computational effort.

The moments $\mu_R^{N,I,0}$ for the living chains and $\mu_P^{M,J,0}$ for the dead chains resp. with the Nth, Mth moment on the chain length, Ith, Jth moment on the number of TDB, and the 0th moment on the branching points are calculated by Equations (2) and (3), respectively:

$$\mu_R^{N,I,0} = \sum_{n=1}^{\infty} n^N \sum_{i=0}^{\infty} i^I \sum_{k=0}^{\infty} R_{n,i,k} \tag{2}$$

$$\mu_P^{M,J,0} = \sum_{m=1}^{\infty} m^M \sum_{j=0}^{\infty} j^J \sum_{l=0}^{\infty} P_{m,j,l} \tag{3}$$

For a complete derivation, we refer to,[10] where the model is called the "TDB double moment model". The complete resulting set of equations is compiled in the Supporting Information. As shown in Equations (4) and (5), closure relations are necessary due to the TDB propagation reaction.

$$\begin{aligned}
\frac{\mu_R^{2,2,0}}{dt} = &\, k_p M \left(2\mu_R^{1,2,0} + \mu_R^{0,2,0}\right) - k_{t,c}\mu_R^{2,2,0}\mu_R^{0,0,0} \\
&- k_{tr,m} M \left(\mu_R^{2,2,0} + \mu_R^{0,0,0}\right) + k_{p,TDB}\left(2\mu_R^{2,1,0}\mu_P^{0,2,0}\right. \\
&- 2\mu_R^{2,1,0}\mu_P^{0,1,0} + \mu_R^{2,0,0}\mu_P^{0,3,0} - 2\mu_R^{2,0,0}\mu_P^{0,2,0} + \mu_R^{2,0,0}\mu_P^{0,1,0} \\
&+ 2\left(\mu_R^{1,2,0}\mu_P^{1,1,0} + 2\mu_R^{1,1,0}\mu_P^{1,2,0} - 2\mu_R^{1,1,0}\mu_P^{1,1,0} + \mu_R^{1,0,0}\mu_P^{1,3,0}\right. \\
&\left.- 2\mu_R^{1,0,0}\mu_P^{1,2,0} + \mu_R^{1,0,0}\mu_P^{1,1,0}\right) + \mu_R^{0,2,0}\mu_P^{2,1,0} + 2\mu_R^{0,1,0}\mu_P^{2,2,0} \\
&\left.- 2\mu_R^{0,1,0}\mu_P^{2,1,0} + \mu_R^{0,0,0}\mu_P^{2,3,0} - 2\mu_R^{0,0,0}\mu_P^{2,2,0} + \mu_R^{0,0,0}\mu_P^{2,1,0}\right)
\end{aligned} \tag{4}$$

$$\begin{aligned}
\frac{\mu_P^{2,2,0}}{dt} = &\, k_{t,c}\left(\mu_R^{2,0,0}\mu_R^{0,2,0} + 2\mu_R^{2,1,0}\mu_R^{0,1,0} + \mu_R^{2,2,0}\mu_R^{0,0,0} + \mu_R^{1,0,0}\mu_R^{1,2,0}\right. \\
&\left.+ 2\mu_R^{1,1,0}\mu_R^{1,1,0} + \mu_R^{1,2,0}\mu_R^{1,0,0}\right) + k_{tr,m} M \mu_R^{2,2,0} \\
&- k_{p,TDB}\mu_R^{0,0,0}\mu_P^{2,3,0}
\end{aligned} \tag{5}$$

The moments $\mu_P^{M,3,0}$ with M = 1,2,3 are the chain length averaged moments and can be estimated by the closure relation from Equation (6):

$$\frac{\mu_P^{M,3,0}\,\mu_P^{M,1,0}}{\mu_P^{M,2,0}\,\mu_P^{M,2,0}} = 1 \tag{6}$$

**ADVANCED
SCIENCE NEWS**

www.advancedsciencenews.com

[M] acro-
olecular
Reaction Engineering

www.mre-journal.de

Full reaction set from Table 1
(m,n): chain length
(i,j): terminal double bonds (TDB)
(k,l): branching points (BP)

$$R_{n,i,k} = R(n, i, k, t)$$
$$P_{m,j,l} = P(m, j, l, t)$$

TDB double moment model

$$\mu_R^{N,I,0} = \sum_{n=1}^{\infty} n^N \sum_{i=0}^{\infty} i^I \sum_{k=0}^{\infty} R_{n,i,k}$$

$$\mu_P^{M,J,0} = \sum_{m=1}^{\infty} m^M \sum_{j=0}^{\infty} j^J \sum_{l=0}^{\infty} P_{m,j,l}$$

$$\mu_R^{N,I,0} = \mu_R^{N,I,0}(t)$$
$$\mu_P^{M,J,0} = \mu_P^{M,J,0}(t)$$

Reduction by assumption of linear relationship between average number of TDB (p) and chain length (m)

$$p = A \cdot m + B$$
$$P_{m,l} = P(m, l, t; A, B)$$
$$R_{n,k} = R(n, k, t; A, B)$$

A,B: unknown Parameters

Calculation of parameters A(t), B(t) using moments of „TDB double moment model"

$$A = \frac{\mu_P^{1,1,0} \mu_P^{0,0,0} - \mu_P^{1,0,0} \mu_P^{0,1,0}}{\mu_P^{2,0,0} \mu_P^{0,0,0} - \mu_P^{1,0,0} \mu_P^{1,0,0}}$$

$$B = \frac{\mu_P^{0,1,0}}{\mu_P^{0,0,0}} - A \cdot \frac{\mu_P^{1,0,0}}{\mu_P^{0,0,0}}$$

$$R_{n,k} = R(n, k, t)$$
$$P_{m,l} = P(m, l, t)$$

Remark: For further notation, the Index for TDB is dropped.

Reducing the number of BP by pseudo-distribution method

$$\phi_n^K = \sum_{k=0}^{\infty} k^K R_{n,k}$$

$$\Psi_m^L = \sum_{l=0}^{\infty} l^L P_{m,l}$$

$$\phi_n^K = \phi^K(n, t)$$
$$\Psi_m^L = \Psi^L(m, t)$$

BP moments as a function of chain length and time

Final set of equations

$$\frac{dI_2}{dt}, \frac{dI}{dt}, \frac{dR_{1,0}}{dt}, \frac{dM}{dt}$$

$$\frac{d\phi_n^0}{dt}, \frac{d\Psi_m^0}{dt}, \frac{d\phi_n^1}{dt}, \frac{d\Psi_m^1}{dt}$$

$$\frac{d\mu_R^{0,0,0}}{dt}, \frac{d\mu_P^{0,1,0}}{dt}, \frac{d\mu_P^{0,2,0}}{dt}, \frac{d\mu_R^{1,0,0}}{dt}, \frac{d\mu_R^{1,1,0}}{dt}, \frac{d\mu_R^{1,2,0}}{dt}, \frac{d\mu_P^{1,0,0}}{dt}, \frac{d\mu_P^{1,1,0}}{dt},$$

$$\frac{d\mu_R^{1,2,0}}{dt}, \frac{d\mu_R^{2,0,0}}{dt}, \frac{d\mu_R^{2,1,0}}{dt}, \frac{\mu_R^{2,2,0}}{dt}, \frac{d\mu_P^{2,0,0}}{dt}, \frac{d\mu_P^{2,1,0}}{dt}, \frac{\mu_P^{2,2,0}}{dt}$$
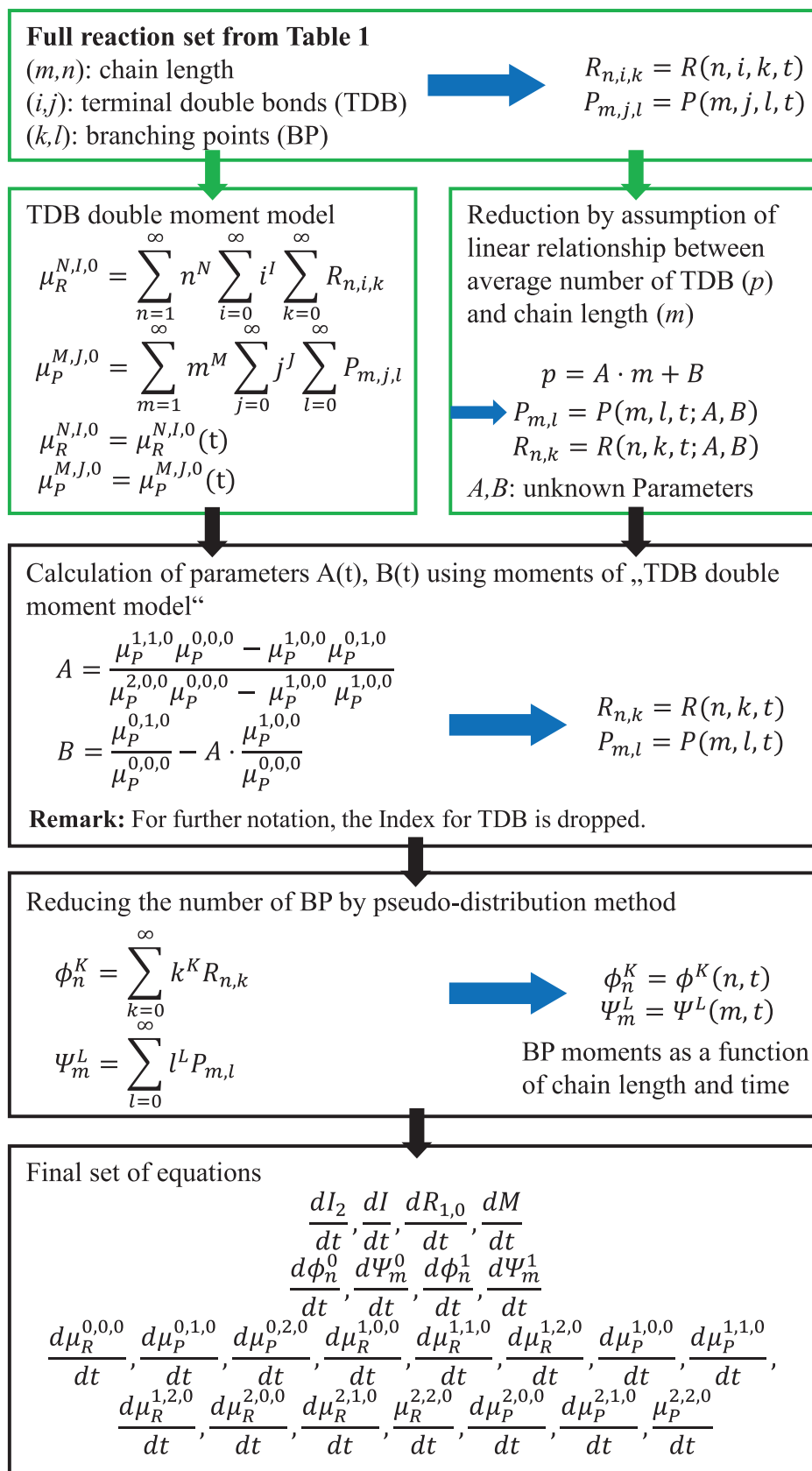
Figure 4. Overview of the different model reduction steps of a full 3D property distribution to a 1D model.

Table 3. Parameter for the reference case that is used for all simulations if not stated otherwise.

Feed	
Monomer weight fraction w^+_{NVP}	0.2
Initiator weight fraction $w^+_{I_2}$	0.0002
Solvent weight fraction $w^+_{H_2O}$	$1 - w^+_{NVP} - w^+_{I_2}$
Feed rate $\dot{m}_F$ [g min^{-1}]	10.38 (resp. in section 3.6: 1.038)
Initial conditions in reactor	
Solvent weight fraction $w^0_{H_2O}$	1
Reactor temperature T_R [°C]	85
Reactor volume V_R [ml]	650
ρ_{H_2O} (85°C) [kg m^{-3}]	959[7]
ρ_{NVP} (85°C) [kg m^{-3}]	989[7]

Using the moments calculated by the "TDB double moment model" allows us to calculate the parameters A and B as follows. B can be determined from the average TDB concentration c^{TDB} per chain calculated from the moments by Equation (7), as demonstrated in[10]:

$$c^{TDB} = \sum_{m=1}^{\infty} \mu_P^{(m),1,0} = A \sum_{m=1}^{\infty} m \cdot \mu_P^{(m),0,0} + B \sum_{m=1}^{\infty} \mu_P^{(m),0,0}$$

$$= A \cdot \mu_P^{1,0,0} + B \cdot \mu_p^{0,0,0} = \mu_P^{0,1,0} \qquad (7)$$

with the 0th and 1st moments on the number of terminal double bonds $\mu_P^{m,0,0}$ resp. $\mu_P^{m,1,0}$ for dead chains. Inserting Equation (7) in Equation (1) results in Equation (8):

$$p(m) = A \cdot \left(m - \frac{\mu_P^{1,0,0}}{\mu_P^{0,0,0}} \right) + \frac{c^{TDB}}{\mu_P^{0,0,0}} = A \cdot \left(m - \frac{\mu_P^{1,0,0}}{\mu_P^{0,0,0}} \right) + \frac{\mu_P^{0,1,0}}{\mu_P^{0,0,0}}$$

$$(8)$$

The parameter A can be calculated from Equation (9):

$$A = \frac{\mu_P^{1,1,0} \mu_P^{0,0,0} - \mu_P^{1,0,0} \mu_P^{0,1,0}}{\mu_P^{2,0,0} \mu_P^{0,0,0} - \mu_P^{1,0,0} \mu_P^{1,0,0}} \qquad (9)$$

For details of the derivation, we refer to Ref. [10]. In Ref. [10], the parameter was calculated once and treated as a constant. In Section 3.6, we demonstrate that the parameter changes during transient operation and propose to calculate the parameter dynamically.

In summary, the full model can be reduced by a linear relation between chain length and the average number of TDBs per molecule. The parameters of this relation can be calculated from a 0D moment model. The elimination of the property coordinate "terminal double bonds" leads to a set of reactions, with two property coordinates: chain length and number of branching points (BP). The corresponding reaction scheme is shown in **Table 4**.

Next, we calculate the moments of the branching points; thus, only the chain length is left as an independent coordinate. The moments of the branching points are determined along the chain length as well. To validate the model, we then compare the simulation results to a class model, which can be seen as a solution

Table 4. Set of reactions after elimination of the TDB property coordinate. Chain length (n,m) and the number of branching points (k,l) are the remaining property coordinates.

Initiator dissociation/Initiation	$I_2 \xrightarrow{k_d} 2f_d I / I + M \xrightarrow{k_p} R_{1,0}$
Propagation	$R_{n,k} + M \xrightarrow{k_p} R_{n+1,k}$
Termination by recombination	$R_{n,k} + R_{m,l} \xrightarrow{k_{t,c}} P_{n+m,k+l}$
Transfer to monomer	$R_{n,k} + M \xrightarrow{k_{tr,M}} P_{n,k} + R_{1,0}$
Propagation of terminal double bonds	$R_{n,k} + P_{m,l} \xrightarrow{p(m) \cdot k_{p,TDB}} R_{n+m,k+l+1}$

to the 2D case (chain length, branching points) if the number of classes is sufficiently high.

Remark: To simplify the notation in the following sections, the first index in subscript or superscripts refers to the chain length (m,n), and the second refers to the number of branching points (k,l). The index for TDB is dropped in subsequent notation.

3.3. Moments of Branching Points

We reduce the property coordinate "branching points" (BP) by taking the moments of the distribution along the BPs, often denoted as the pseudodistribution method.[12]

The Kth resp. Lth branching moments are defined in Equation (10) for living chains and in Equation (11) for dead chains:

$$\phi_n^K = \sum_{k=0}^{\infty} k^K R_{n,k} \qquad (10)$$

$$\Psi_m^L = \sum_{l=0}^{\infty} l^L P_{m,l} \qquad (11)$$

The first moments, ϕ_n^1 and Ψ_m^1 are the concentrations of BP in living or dead chains of length (n,m). The chain length moments for living chains are defined by Equation (12) resp. for the dead chain in Equation (13).

$$\mu_R^{N,K=0} = \sum_{n=0}^{\infty} n^N \phi_n^0 = \sum_{n=0}^{\infty} n^N \sum_{k=0}^{\infty} R_{n,k} \qquad (12)$$

$$\mu_P^{M,L=0} = \sum_{m=0}^{\infty} m^M \Psi_m^0 = \sum_{m=0}^{\infty} m^M \sum_{l=0}^{\infty} P_{m,l} \qquad (13)$$

Application of the weighted summation over branching points for propagation and transfer to monomer reaction is straightforward, while termination by combination reaction needs more consideration due the occurrence of a double sum due to the combination of two molecules. The propagation of terminal double bonds also needs to be considered in more detail. The complete derivation of moment equations is lengthy and detailed in the Supporting Information. An example of the contribution to the overall balance for the propagation of TDB is shown in Equation (14) for living chains and for dead chains in Equation (15). The moment equations for the living chains should be understood as follows: The terms with a negative sign indicate the consumption of living chains, whereas a positive sign indicates the

ADVANCED
SCIENCE NEWS

www.advancedsciencenews.com

[M] acro-
molecular

Reaction Engineering

www.mre-journal.de

formation of a living chain with the formation of a BP. It is important to note here that the reaction rate is multiplied by the linear correlation between the average number of TDBs per molecule and the chain length. The moment equations for dead chains only describe the consumption of dead chains and can be calculated straight forward.

$$
\frac{d\phi_n^K}{dt} + = k_{p,TDB} \sum_{k=0}^{\infty} k^K \left(-R_{n,k} \sum_{m=1}^{\infty} \sum_{l=0}^{\infty} p(m) P_{m,l} \right.
$$
$$
\left. + \sum_{m=1}^{n-1} \sum_{l=0}^{k-1} p(m) P_{m,l} R_{n-m,k-l-1} \right)
$$
$$
= k_{p,TDB} \left(-\phi_n^K \sum_{m=1}^{\infty} p(m) \Psi_m^0 \right.
$$
$$
+ \sum_{m=1}^{n-1} \sum_{l=0}^{\infty} p(m) P_{m,l} \left(\sum_{k=l+1}^{\infty} k^K R_{n-m,k-l-1} \right) \right)
$$
$$
= k_{p,TDB} \left(-\phi_n^K \sum_{m=1}^{\infty} p(m) \Psi_m^0 \right.
$$
$$
\left. + \sum_{m=1}^{n-1} \sum_{l=0}^{\infty} p(m) P_{m,l} \left(\sum_{k=0}^{\infty} (k+l+1)^K R_{n-m,k} \right) \right) \tag{14}
$$

$$
\frac{d\Psi_m^L}{dt} + = -k_{p,TDB} \, p(m) \sum_{l=0}^{\infty} l^L P_{m,l} \sum_{n=1}^{\infty} \sum_{k=0}^{\infty} R_{n,k}
$$
$$
= -k_{p,TDB} \, p(m) \, \Psi_m^L \mu_R^{0,K=0} \tag{15}
$$

To evaluate the number of branching points as a function of chain length, the zeroth and the first moments of the dead and living chains must be considered in the model. The contribution to the dynamics of the zeroth moments for the propagation of the TDB reaction is evaluated in Equation (16) for living chains and for dead chains in Equation (17). The zeroth moments are obtained straight forward by inserting zero for K resp. L and the transformation to moments.

$$
\frac{d\phi_n^0}{dt} + = k_{p,TDB} \left(-\phi_n^0 \sum_{m=1}^{\infty} p(m) \, \Psi_m^0 \right.
$$
$$
\left. + \sum_{m=1}^{n-1} \sum_{l=0}^{\infty} p(m) \, P_{m,l} \left(\sum_{k=0}^{\infty} (k+l+1)^0 R_{n-m,k} \right) \right)
$$
$$
= k_{p,TDB} \left(-\phi_n^0 \sum_{m=1}^{\infty} p(m) \, \Psi_m^0 + \sum_{m=1}^{n-1} p(m) \Psi_m^0 \phi_{n-m}^0 \right) \tag{16}
$$

$$
\frac{d\Psi_m^0}{dt} + = -k_{p,TDB} \, p(m) \, \Psi_m^0 \mu_R^{0,K=0} \tag{17}
$$

The contribution of this reaction to the first moments is shown in Equation (18) for living chains and for dead chains in Equation (19). To obtain the first moments, K and L are set to one. The

first moment then reads:

$$
\frac{d\phi_n^1}{dt} + = k_{p,TDB} \left(-\phi_n^1 \sum_{m=1}^{\infty} p(m) \Psi_m^0 \right.
$$
$$
\left. + \sum_{m=1}^{n-1} \sum_{l=0}^{\infty} p(m) P_{m,l} \sum_{k=0}^{\infty} (k+l+1)^1 R_{n-m,k} \right)
$$
$$
= k_{p,TDB} \left(-\phi_n^1 \sum_{m=1}^{\infty} p(m) \Psi_m^0 + \sum_{m=1}^{n-1} p(m) \left(\sum_{l=0}^{\infty} l P_{m,l} \phi_{n-m}^0 \right. \right.
$$
$$
\left. \left. + \sum_{k=0}^{\infty} k \Psi_m^0 \, R_{n-m,k} + \Psi_m^0 \phi_{n-m}^0 \right) \right)
$$
$$
= k_{p,TDB} \left(-\phi_n^1 \sum_{m=1}^{\infty} p(m) \Psi_m^0 + \sum_{m=1}^{n-1} p(m) \left(\Psi_m^1 \phi_{n-m}^0 \right. \right.
$$
$$
\left. \left. + \Psi_m^0 \phi_{n-m}^1 + \Psi_m^0 \phi_{n-m}^0 \right) \right) \tag{18}
$$

$$
\frac{d\Psi_m^1}{dt} + = -k_{p,TDB} \, p(m) \, \Psi_m^1 \mu_R^{0,K=0} \tag{19}
$$

The overall zeroth and first moments of branching points for a CSTR are as follows:

$$
\frac{d\phi_n^0}{dt} = k_p M \left(-\phi_{n-1}^0 + \phi_n^0 \right) - k_{t,c} \mu_R^{0,K=0} \phi_n^0 - k_{tr,M} M \phi_n^0
$$
$$
+ k_{p,TDB} \left(-\phi_n^0 \sum_{m=1}^{\infty} p(m) \, \Psi_m^0 + \sum_{m=1}^{n-1} p(m) \, \Psi_m^0 \phi_{n-m}^0 \right) - \frac{\dot{V}^+}{V_R} \phi_n^0 \tag{20}
$$

$$
\frac{d\Psi_m^0}{dt} = \frac{1}{2} k_{t,c} \sum_{n=1}^{m-1} \phi_n^0 \phi_{m-n}^0 + k_{tr,M} M \phi_m^0 - k_{p,TDB} p(m) \Psi_m^0 \mu_R^{0,K=0}
$$
$$
- \frac{\dot{V}^+}{V_R} \Psi_m^0 \tag{21}
$$

$$
\frac{d\phi_n^1}{dt} = k_p M \left(-\phi_{n-1}^1 + \phi_n^1 \right) - k_{t,c} \mu_R^{0,K=0} \phi_n^1 - k_{tr,M} M \phi_n^1
$$
$$
+ k_{p,TDB} \left(-\phi_n^1 \sum_{m=1}^{\infty} p(m) \Psi_m^0 + \sum_{m=1}^{n-1} p(m) \left(\Psi_m^1 \phi_{n-m}^0 \right. \right.
$$
$$
\left. \left. + \Psi_m^0 \phi_{n-m}^1 + \Psi_m^0 \phi_{n-m}^0 \right) \right) - \frac{\dot{V}^+}{V_R} \phi_n^1 \tag{22}
$$

$$
\frac{d\Psi_m^1}{dt} = k_{t,c} \sum_{n=1}^{m-1} \phi_n^1 \phi_{m-n}^0 + k_{tr,M} M \phi_m^1 - k_{p,TDB} p(m) \Psi_m^1 \mu_R^{0,K=0}
$$
$$
- \frac{\dot{V}^+}{V_R} \Psi_m^1 \tag{23}
$$

**ADVANCED
SCIENCE NEWS**

www.advancedsciencenews.com

[M] acro-
molecular
Reaction Engineering

www.mre-journal.de

$\dot{V}^+$ describes the influx, and V_R describes the volume of the reactor. The model is linear in the property coordinate of the number of branching points. Therefore, no closure relation for the branching point property coordinate is needed, and only the zeroth and first branching point moments are evaluated because higher moments do not provide additional information. In what follows, we refer to this model as the "BP moment model".

3.4. Class Model for Chain Length and Branching Points

The class approach allows to calculate 2D distributions. Usually, one property is treated as a continuous variable (here: chain length), while the second property coordinate is treated as a discrete variable (here: branching points). For each number of branching points, a balance equation is needed, which is called a "class."[13] This is only feasible if the distribution of the discrete variable decays sufficiently fast and the number of classes can be kept low.

For example, $R_{n,1}$ is a living polymer of chain length (n) carrying one branching point, and $P_{m,2}$ is a dead polymer of chain length (m) carrying two branching points. The whole reaction scheme presented in **Table 4** can be derived by assigning numbers to the second property coordinate. To describe the propagation of terminal double bonds, for example, the number of branching points is summed up and added by one since one branching point is additionally created during the reaction, which is shown in Equation (24):

$$R_{n,1} + P_{m,2} \xrightarrow{p(m) \cdot k_{p,TDB}} R_{n+m,4} \tag{24}$$

The BP class model yields exact solutions if the number of branching points (k,l) is unlimited. For practical reasons, however, a cutoff value is used, which limits the number of BPs to values typically lower than 10 to reduce the computational effort. If a reaction results in higher numbers of BP than 10, they are combined in the cutoff value of 10.

A class model with a cutoff value of 10 is applied here, which will be referred to as the "BP class model". However, this model only works satisfactorily if fewer than 10 branching points are relevant. Nevertheless, the computational effort is very high. For these reasons, the class model will only serve to validate the "BP moment model".

3.5. Comparison of the BP Moment Model and the BP Class Model

To validate the derivation and implementation of the BP moment and BP class models, both models are compared for the reference case defined in Table 3. The most important information that can be extracted from both models is the average number of branching points per chain of length (m) calculated by Equation (25):

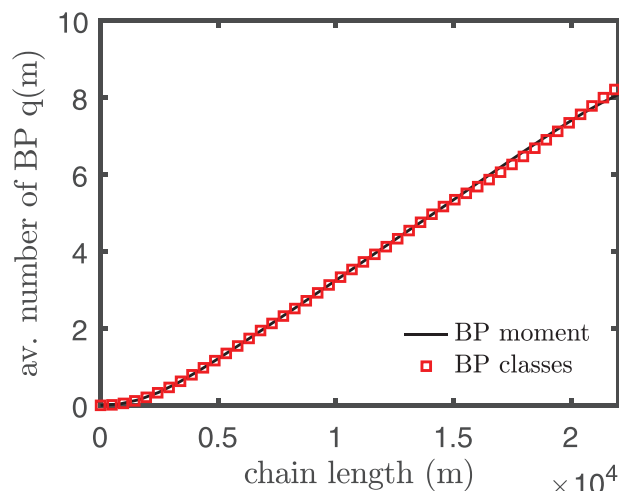$$q(m) = \frac{\Psi_m^1}{\Psi_m^0} \tag{25}$$

Figure 5. Comparison of the average number of branching points q(m) as a function of the chain length for the BP moment and class model for the stationary reference case.
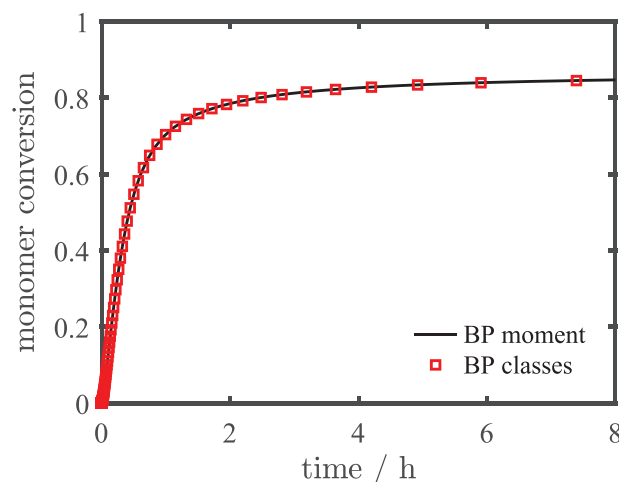

Figure 6. Comparison of the average branching points per molecule for the BP moment and class model for the reference case.

as well as the average number of branching points per molecule defined in Equation (26), which is the corresponding ratio of the integrals over all chain lengths:

$$\frac{\sum_m \Psi_m^1}{\sum_m \Psi_m^0} = \frac{c^{BP}}{\mu_P^{0,L=0}} \tag{26}$$

Figure 5 shows the average number of BP per chain of length (m). After an initial delay, the number of branching points correlated linearly with chain length. **Figure 6** shows the average number of branching points after start-up of the CSTR. During the first hours, the number of branching points rises and levels off when approaching the steady state.

To validate the BP moment model, a comparison of the normalized gel permeation chromatography (GPC) distribution for both models was made, which is shown in **Figure 7**. Both models show indistinguishable results for the GPC distribution as
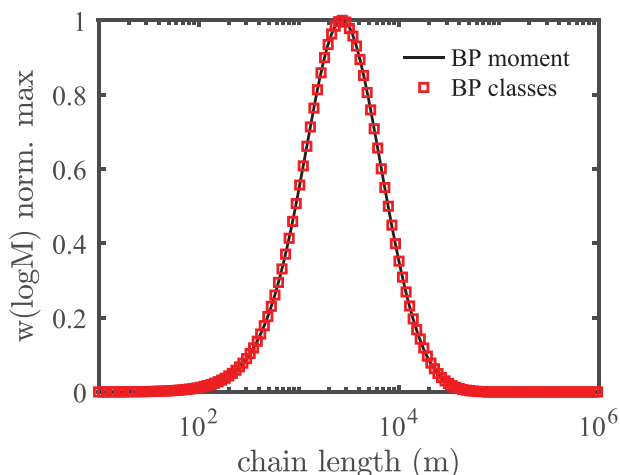
**ADVANCED
SCIENCE NEWS**
www.advancedsciencenews.com

[M]acro-
molecular
Reaction Engineering
www.mre-journal.de

Figure 7. Comparison of the normalized GPC distribution for the BP moment and class model for the stationary reference case.
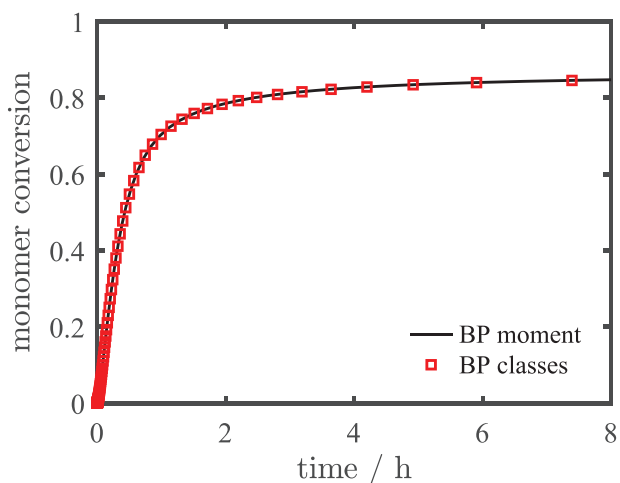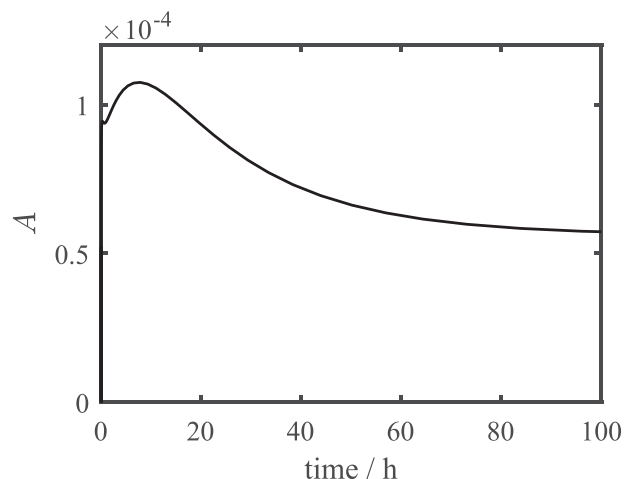

Figure 9. Time dependence of parameter A for the modified reference case calculated with the TDB double moment model.
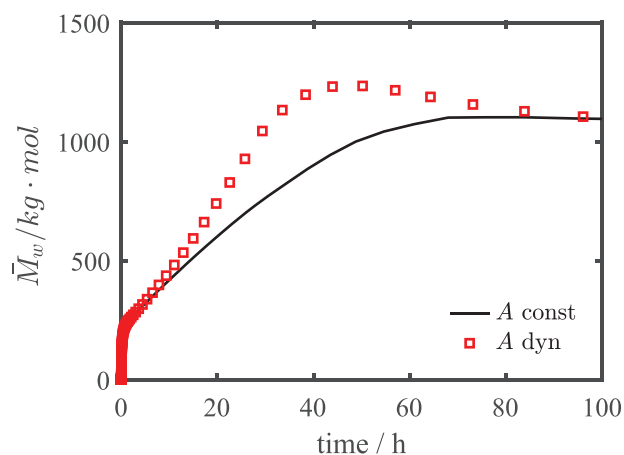

Figure 8. Comparison of the evolution of monomer conversion for the BP moment and class model for the reference case.

Figure 10. Comparison of the average molecular weight as a function of time for a constant A and the dynamically calculated A calculated with the BP moment model acc. to Equation (1) for the modified reference case.

well as the evolution of monomer conversion, which is shown in **Figure 8**.

The two different models for calculation of the branching point distribution were compared and show excellent agreement.

3.6. Dynamic Calculation of Parameter A in the BP Moment Model

In Section 3.1, we have shown that the parameters of the linear relation between chain length and number of terminal double bonds can be calculated from a 0D moment model. In[10] parameter A was calculated for steady-steady and parameter B by using a massless counter variable to track the total number of terminal double bonds c^{TDB}.

Thus, a constant A provides correct results for the stationary case but is not a good approximation during transient operations such as startup and shutdown. Therefore, we propose to continuously adapt parameter A by calculating the moment model ("TDB double moment model") and the BP moment model in parallel.

An additional advantage of combining the two models is the ability to change the recipe without reparameterization of A. To demonstrate the advantage of continuous adaptation of parameter A (and B), a start-up of a CSTR is calculated with a very low feed rate ($\dot{m}_F$ = 1.038 g min–1) and thus a high residence time of τ = 10 h. **Figure 9** shows the evolution of A during the transition to steady-state operation, and **Figure 10** is the mass averaged polymer weight for a constant (stationary value $A = 5.62 \times 10^{-5}$ from Figure 9) and a continuously adapted value of A.

The molecular weight with a constant value for A is underestimated because the steady state value for A is lower than the dynamically calculated value. The stationary state of the reaction system was reached after 100 h of reaction time. A dynamically calculated A depends on the state of the reaction system, and therefore, it takes even longer to reach a steady state.

Additionally, the normalized GPC distribution at different times is shown in **Figure 11**a-c to demonstrate the dynamic behavior of the CSTR and the benefit of calculating distributions such as the GPC distribution simultaneously. The previously mentioned finding that the steady state for a dynamically calcu-
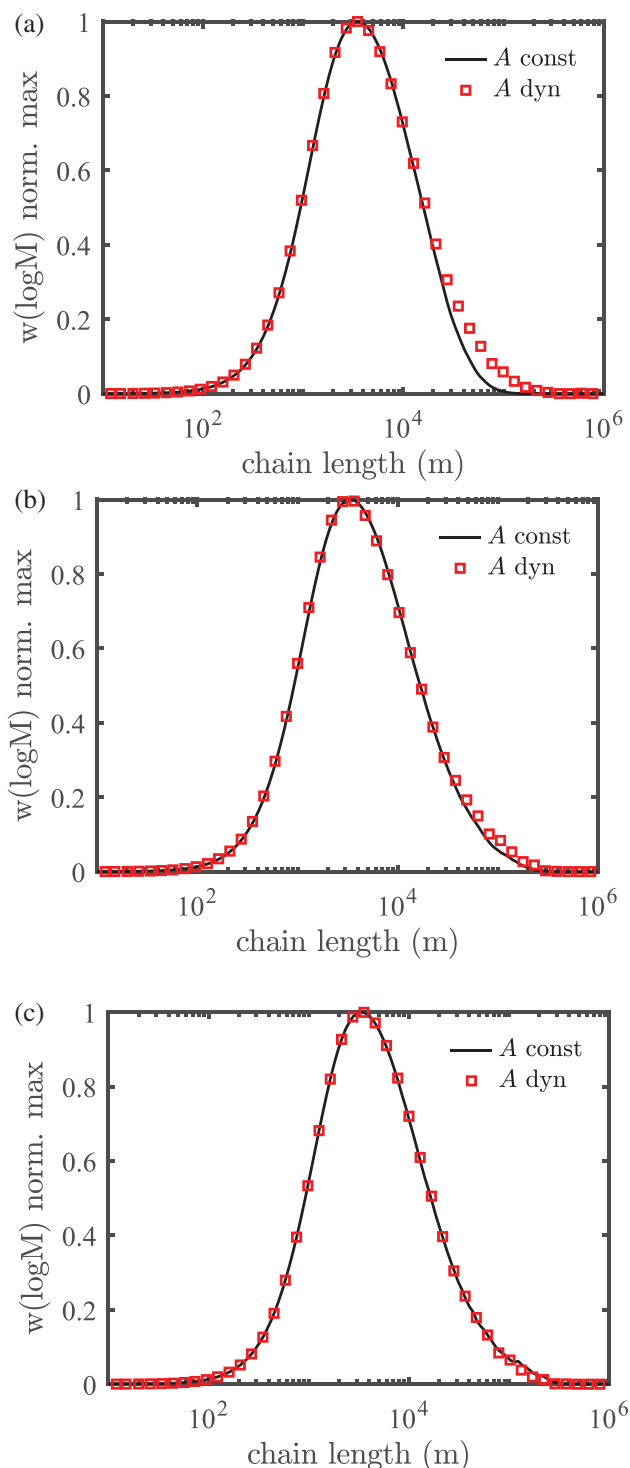
ADVANCED
SCIENCE NEWS

www.advancedsciencenews.com

[M]acro-
molecular
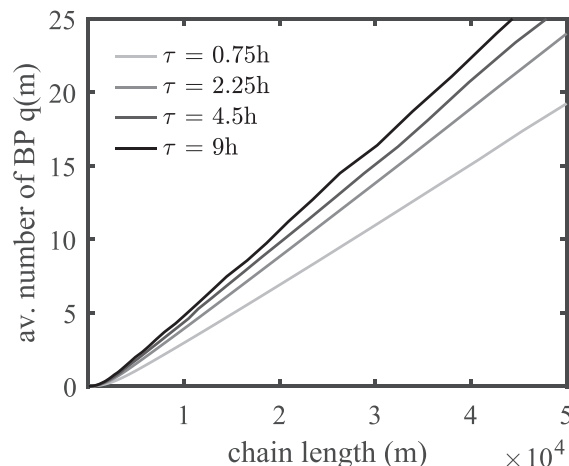Reaction Engineering

www.mre-journal.de

Figure 12. Comparison of the average number of branching points depending on the chain length for different residence times. Small variations are due to the numerical accuracy.

Figure 11. Comparison of the normalized GPC distribution for the BP moment calculated with a constant and a dynamically calculated A for the modified reference case. a) Results after 30h of reaction time. b) Results after 60h of reaction time. c) Results after 100h of reaction time.

lated A takes longer can also be seen in Figure 11b. The GPC distribution between a dynamically calculated A and a fixed value for A still deviates after 60 h, while after 100 h, both distributions agree. Clearly, a constant value of An introduces some error during the transition to the steady state.

4. Results

Using the 0D "TDB double moment model" (Equations (2)–(5)) together with the "BP moment model" (Equations (20)–(23)) allows us to calculate the molecular weight distribution together with the moments of the branching points. **Figure 12** shows the average number of branching points as a function of chain length for different residence times in a CSTR. The number of branches increases approximately linearly with the chain length. Long polymers react more often with polymers containing terminal double bonds and consequently have more branching points. With increasing residence time, the number of branching points per molecule also increases. This can be explained by the lower monomer and initiator concentrations, which favors the propagation of TDBs, and more branching points are formed. **Figure 13** shows the time-dependent average BP per molecule. The stationary number of branching points increases with residence times, while the initial slope decreases slightly.

The increase in the average number of branching points is directly related to the formation of long polymer chains with increasing residence time. Then, side reactions such as transfer to monomers and subsequent propagation of TDB become more important. **Figure 14** presents the number of branches per 1000 repeat units as a function of molecular weight in a double logarithmic plot. This type of diagram is useful for comparison with experimental data since most analytical methods determine branches per 100 or 1000 repeat units.[14] A low residence time leads to short chains that carry a relatively low number of branching points. High residence times, on the other hand, lead to the formation of polymers with a high molecular weight and with a high content of branches.
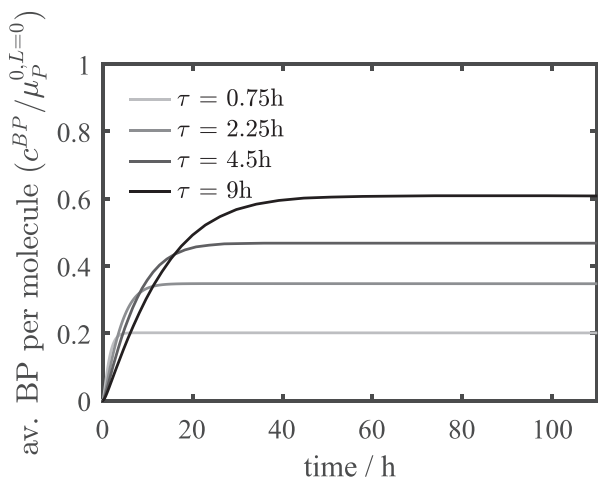
ADVANCED
SCIENCE NEWS
www.advancedsciencenews.com

acro-
[M] olecular
Reaction Engineering
www.mre-journal.de

Figure 13. Comparison of the average number of branching points per molecule depending on time for different residence times.
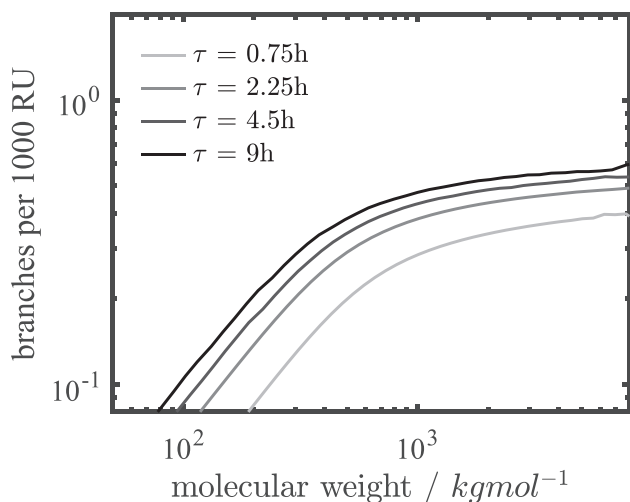

Figure 14. Comparison of the average number of branching points per 1000 repeat units depending on molecular weight for different residence times.
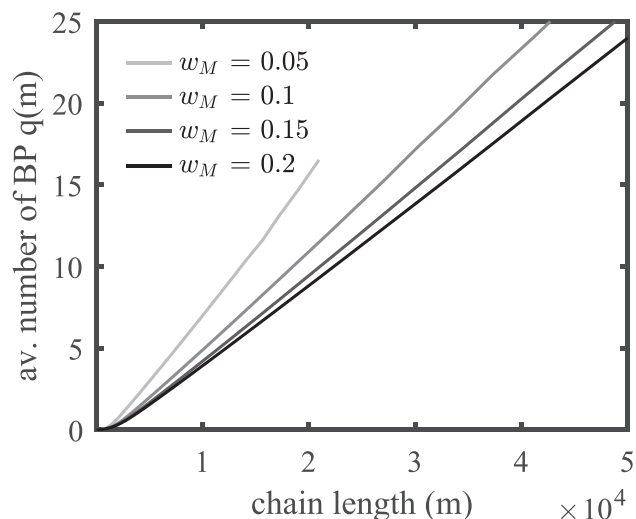

Figure 15. Comparison of the average number of branching points depending on the chain length for different monomer concentrations with an average residence time $\tau = 2.25$ h.
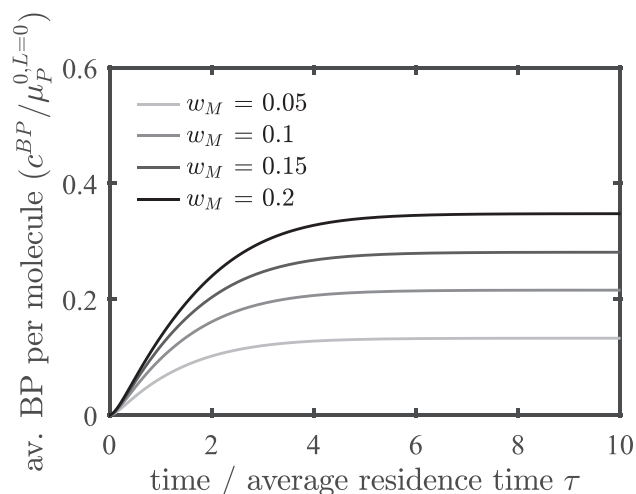

Figure 16. Comparison of the average number of branching points per molecule depending on time for different monomer concentrations with an average residence time $\tau = 2.25$ h.

In the following, the impact of monomer concentration on the branching distribution is investigated. The reference case from Table 3 was modified with respect to the feed rate and monomer concentration. The modified parameters are listed in **Table 5**.

Figure 15 shows the average number of branching points for different monomer concentrations along the chain length. While

Table 5. Parameters for the investigation of the influence of the monomer concentration.

Feed	
Monomer weight fraction w_{NVP}^+	0.05–0.2
Initiator weight fraction $w_{I_2}^+$	0.0002
Solvent weight fraction $w_{H_2O}^+$	$1-w_{NVP}^+ - w_{I_2}^+$
Feed rate $\dot{m}_F$ [g min^{-1}]	4.6

the average chain length decreases with monomer concentration, the number of branches per molecule increases. At high monomer conversion, side reactions such as TDB propagation become more favorable, and more branching points are formed. The number of branching points for a monomer concentration of $w_M = 0.05$ is shown in Figure 15 only up to a certain chain length because the concentration of longer chains is very low and numerical noise occurs.

Figure 16 shows that at higher monomer concentrations, the average number of branching points per molecule increases. This is a consequence of increasing chain length.

Figure 17 presents the behavior of branching points per 1000 repeat units depending on the molecular weight for different monomer concentrations. A low monomer content leads to short chains and generally to a low molecular weight while carrying a relatively high number of branching points. Higher monomer
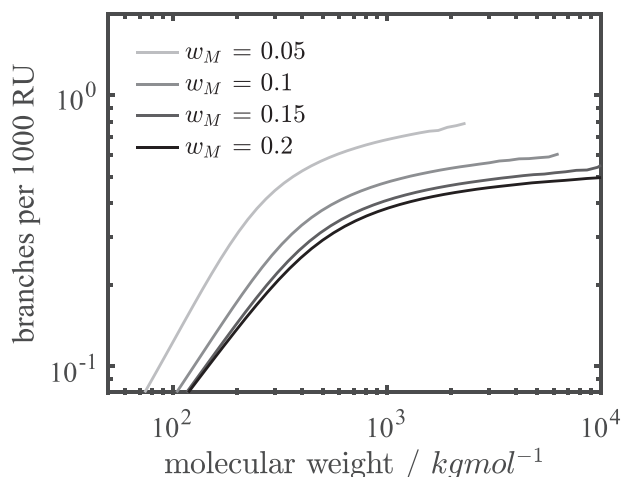
Figure 17. Comparison of the average number of branching points per 1000 repeat units depending on molecular weight for different monomer concentrations with an average residence time $\tau = 2.25$ h.

content, on the other hand, leads to polymers with a lower content of branches compared to lower monomer content.

5. Conclusion

To describe the onset of fouling for polymerization on N-vinylpyrrolidone, a detailed kinetic scheme was developed. Rigorous simulation using the detailed kinetics would require a 3D property space: chain length, terminal double bonds (TDB) and branching points (BP). In this contribution, we extend the approach of Zander[10] in two directions. First, the parameters of the linear relation between chain length and number of TDBs are dynamically adapted by using a 0D moment model, which is calculated in parallel. Second, by calculating the chain length distributed moments of the branching points, a 1D model for the number of branching points along the chain length was derived. Simulation of this 1D model (termed the BP moment model) together with the 0D model allows calculation of the polymer microstructure (chain length distribution, number of BP and TDB as a function of chain length) during transient operation of a reactor. The new model was compared to a computationally expensive class model with full accordance.

To separate the effects of hydrodynamics and kinetics, we used the new model to calculate polymer properties during the transition of a CSTR to the steady state and showed the impact of residence time and monomer concentration.

In future work, we will compare the simulated branching point distribution to experimental data.

Supporting Information

Supporting Information is available from the Wiley Online Library or from the author.

[1] J. Urrutia, A. Peña, J. M. Asua, *Macromol. React. Eng.* **2017**, *11*, 1600043.
[2] D. Kohlmann, M.-C. Chevrel, S. Hoppe, D. Meimaroglou, D. Chapron, P. Bourson, C. Schwede, W. Loth, A. Stammer, J. Wilson, P. Ferlin, L. Falk, S. Engell, A. Durand, *Macromol. React. Eng.* **2016**, *10*, 339.
[3] C. Bernstein, "Methoden zur Untersuchung der Belagsbildung in chemischen Reaktoren." Hamburg, **2017**.
[4] M. Stach, I. Lacík, D. Chorvát, M. Buback, P. Hesse, R. A. Hutchinson, L. Tang, *Macromolecules* **2008**, *41*, 5174.
[5] L. Uhelská, D. Chorvát, R. A. Hutchinson, S. Santanakrishnan, M. Buback, I. Lacík, *Macromol. Chem. Phys.* **2014**, *215*, 2327.
[6] J. Schrooten, M. Buback, P. Hesse, R. A. Hutchinson, I. Lacík, *Termination kinetics of 1−vinylpyrrolidin−2−one radical polymerization in aqueous solution*, *212*, 1400–1409.
[7] S. Santanakrishnan, L. Tang, R. A. Hutchinson, M. Stach, I. Lacík, J. Schrooten, P. Hesse, M. Buback, *Macromol. React. Eng.* **2010**, *4*, 499.
[8] F. Haaf, A. Sanner, F. Straub, *Polym. J.* **1985**, *17*, 143.
[9] P. Deglmann, M. Hellmund, K.-D. Hungenberg, U. Nieken, C. Schwede, C. Zander, *Macromol. React. Eng.* **2019**, *13*, 1900021.
[10] C. Zander, K.-D. Hungenberg, T. Schall, C. Schwede, U. Nieken, *Macromol. React. Eng.* **2020**, *14*, 2000009.
[11] J. Schrooten, M. Buback, P. Hesse, R. A. Hutchinson, I. Lacík, *Macromol. Chem. Phys.* **2011**, *212*, 1400.
[12] P. D. Iedema, M. Wulkow, H. C. J. Hoefsloot, *Macromolecules* **2000**, *33*, 7173.
[13] P. D. Iedema, H. C. J. Hoefsloot, *Macromolecules* **2003**, *36*, 6632.
[14] J. C. Randall, *J. Macromol. Sci. Part C* **1989**, *29*, no. 2–3, pp. 201.